

## **Steering Angle Sensorless Control for Four-wheel Steering Vehicle via Sliding Mode Control Method**

**Abstract:** This paper presents a new sensorless control method for four-wheel steering vehicles. Compared to the existing sensor-based control, this approach improved dynamic stability, manoeuvrability, and robustness in case of malfunction of the front steering angle sensor. It also provided a software redundancy and backup solution, as well as improved fault tolerance. The strategy of the sensorless control is based on the sliding mode method to estimate the replacement of the front steering input from the errors between the vehicle's measured and desired values of the vehicle's sideslip angle and yaw rate. The simulation results demonstrate that the observer effectively estimated the front-wheel steering angle at both low and high speeds scenarios in the cornering and lane change manoeuvres. Furthermore, the sensorless control approach can achieve equivalent control performances to the sensor-based controller including a small and stable yaw rate response and zero sideslip angle. The results of the study offer a potential solution for improving manoeuvrability, stability, and sensor fault tolerance of four-wheel steering vehicles.

**Keywords:** four-wheel steering; steering control; sensorless control; observer; sliding mode control; steering stability

### **1 Introduction**

As part of an active chassis control framework, a four-wheel-steering (4WS) system is a key technology for improving the active safety and manoeuvrability performance of vehicles in general usage (Shibahata, 2005). With the rapid development of in-wheel motor electric vehicles, the automobile industry has shown a lot of interest in the 4WS technology as a development platform. The manoeuvrability and stability of a vehicle are

critical during driving, otherwise, and lack thereof can result in safety hazards. Conventional front-wheel steering (FWS) vehicle is prone to sideslip or tailspin when turning, as their rear wheels are in passive working mode and follow the direction of the front wheels' angle. In contrast, the 4WS system can actively control the rear-wheel steering angle both in terms of size and direction, which can achieve manoeuvrability at low speed and stability at high speed by cooperating with the front-wheel steering angle. Nevertheless, the 4WS vehicle dynamics in the real world are nonlinear and time-varying, with strongly coupled state variables due to modelling' errors, external disturbances, and changes in load and road conditions. To address these challenges, a robust control scheme is required to realise the 4WS vehicle manoeuvrability and stability performance.

The original 4WS system was designed with the principle of actively controlling the rear wheel angle to achieve the desired tracking and stability performance. Many control systems have been developed for active rear-wheel steering (ARS) including the combination control of feedforward and feedback (Yu et al., 2018), optimization control (Du et al., 2022), robust control (Xu et al., 2019, Zhao et al., 2018), model predictive control (Arslan and Sever, 2019), neural network control (Li et al., 2021) and fuzzy control (Cao and Qiao, 2017) have been applied. Their results show that appropriate sideslip angles and yaw rate could be achieved by regulating the rear steering angles, which could increase the vehicle's stability at high speeds and manoeuvrability at low speeds. Another efficient chassis control method, direct yaw-moment control (DYC), has been applied in the vehicle dynamics control system and was presented to enhance driving stability. The DYC technique used yaw rate, which is dependent on the tire longitudinal force, to control the yaw motion of the vehicle. At present there is much research on DYC including robust control ( Yu et al., 2013), decoupling control method (Jiang et al., 2020), fuzzy control (Xianjian Jin et al., 2018), and sliding mode control (SMC) (Asiabar and Kazemi, 2019). However, the dynamics between tire and ground are nonlinear. The change in the steering parameter would have an impact on the vehicle state's control performance (Cordeiro et al., 2019). As a result, with the use of ARS or DYC, it can be challenging to achieve satisfactory outcomes, especially in situations when high speed or swerving are involved. The requirement for a vehicle stability control system is

brought on by the integrated control strategy between the DYC and other active steering technologies (Ge et al., 2021). Wang et al. (2020) proposed an optimal coordinated control based on the integration control of ARS and DYC. A decoupling control approach was presented by Liang et al. (2020) to regulate the involvement of active steering and DYC for a four-wheel independent steering vehicle to improve the lateral dynamics performance in high-speed conditions. Zhang et al. (2022) introduced an optimal control strategy with feedback control to control the yaw rate and centroid cornering angle by adjusting the steering angles. Furthermore, robust controllers were illustrated recently to improve the tracking ability, which integrated the DYC control method with the 4WS system containing front and rear steering angles (Hang et al., 2019). These optimization algorithms or robust control could be costly in the implementation due to the use of high-dimensional matrices. The compromise solution is supposed to design control schemes that are robust but do not require a large computational load.

As a strong robust approach, the SMC strategy benefits from the simple algorithm, and reliability for a nonlinear model with uncertainty and external disturbances. Because the sliding mode motion in the variable space is insensitive to parameter changes and disturbances, the coupling within the system can be eliminated (Utkin, 1992). Motivated by the above discussions, an SMC algorithm that integrated the ARS and DYC has been proposed for the 4WS vehicle in our previous work (Yuan et al., 2017). The control variables, including the sideslip angle and yaw rate of the centre of gravity (COG), can each achieve their desired goals assuming a 15% increase in the vehicle's mass and inertia. The simulation results showed significant improvements in the vehicle's manoeuvrability and stability compared to the FWS control under different steering input signals and vehicle velocities.

The control strategies mentioned above improved the vehicle's handling and stability performance but ignored the effects of the steering angle's sensor failure. All the above control schemes inevitably require the input of the front steering angle which is generally fed by a mechanical steering device or steer-by-wire. The front steering angle sensor is a crucial measurement tool for the vehicle control system, although the noise will be

input into the system together. It could deliver feedback to the controller through an electric signal. However, due to less coordination of the assembled parts or vibrations on a bumpy road, the sensor may become faulty and stop functioning. At this point, the vehicle stability would decrease because the stability control system would not work properly. To address this issue, one possible solution is to use an estimated state of the front steering angle sensor as a substitute, effectively replacing hardware redundancy with software redundancy (Zhang and Zhao, 2018). Furthermore, indirect estimation of the state will be a cost-effective method instead of measurement (Zhang et al., 2016). To the best of our knowledge, there is no sensorless control with a steering angle observer for the 4WS system in the literature except that the steering sensor observer was used for fault detection (Boukhari et al., 2018; Li et al., 2017).

The present work aims to improve the 4WS vehicle's overall manoeuvrability and stability performance safely and reliably based on the SMC strategy that integrated the ARS and DYC. Considering the possible failure of the sensor of the front steering angle, an observer was designed to estimate its state as a backup for the proposed control strategy. Using Lyapunov's theory, the system is proved to be asymptotically stable when the disturbance boundary coefficient is greater than one in the presence of parameter disturbances. On the foundation of the previous study, the main contributions include: (1) A designed observer is proposed to estimate the steering angle of the front wheel, which can improve the robustness in the event of sensor failure as a redundancy. (2) The performance of the sensorless sliding mode controller is comparable to that of the sensor-based method in the 4WS vehicle's manoeuvrability and stability. The results are encouraging and show the significance of sensorless control research for vehicle dynamic analysis.

The remainder of the paper is organized as follows. First, Section 2 presents the 4WS vehicle dynamic models. A seven-degree of freedom (DOF) model is presented as the plant of control, which was linearized to a 2-DOF lateral model. In this case, the control error could be calculated by comparing the linear and ideal steering reference models. The design process of the sliding mode strategy with an observer of the steering angle will be shown in section 3. The numerical simulation has been implemented and analysed in Section 4. Lastly,

Section 5 concludes this work, highlighting that the simulation results show the method to be feasible and effective.

## 2 4WS vehicle dynamic model and reference model

### 2.1 7- DOF dynamic model

The 4WS steering systems have been modelled using the 7-DOF steering model illustrated in Figure 1. Regardless of body tilt, the 4WS vehicle is considered to be a rigid body with symmetrical, uniformly distributed masses, and its mass is shown by  $m$ . The centre of gravity of the vehicle body serves as the coordinate origin of the model. The forward direction of the vehicle is the positive direction of the x-axis. The y-axis is used to describe the lateral movement of the vehicle, which is perpendicular to the x-axis and forms a horizontal plane with the x-axis. The sideslip angle ( $\beta$ ) and the yaw rate ( $\dot{\gamma}$ ), respectively, characterize the lateral and yaw movements. The 7-DOF dynamic model can be derived as the following:

$$\begin{cases} m(\dot{v}_x - v_y \dot{\gamma}) = (F_{x1} + F_{x2}) \cos \delta_f - (F_{y1} + F_{y2}) \sin \delta_f + (F_{x3} + F_{x4}) \cos \delta_r - (F_{y3} + F_{y4}) \sin \delta_r \\ m(\dot{v}_y + v_x \dot{\gamma}) = (F_{x1} + F_{x2}) \sin \delta_f + (F_{y1} + F_{y2}) \cos \delta_f + (F_{x3} + F_{x4}) \sin \delta_r + (F_{y3} + F_{y4}) \cos \delta_r \\ I_z \dot{\gamma} = a(F_{y1} + F_{y2}) \cos \delta_f - b(F_{y3} + F_{y4}) \cos \delta_r + 0.5W[(F_{y1} - F_{y2}) \sin \delta_f + (F_{y3} - F_{y4}) \sin \delta_r] + M \\ J_{wi} \dot{\omega}_i = M_{di} - F_{xi} R - M_{bi} \quad (i = 1, 2, 3, 4) \end{cases} \quad (1)$$

where  $v_x$  and  $v_y$ , respectively, are components in the x-axis and y-axis of the centroid velocity  $V$ ,  $I_z$  represents the z-axis yaw moment of inertia,  $a$  or  $b$  are the distances between the COG and the front axis or rear axis respectively, the wheelbase, or  $L$ , equals the sum of  $a$  and  $b$ ,  $\delta_f$  and  $\delta_r$  are front and rear steering angles of wheels,  $F_{xi}$  and  $F_{yi}$  indicates the  $i$ th ( $i=1,2,3,4$ ) tire's longitudinal and lateral force,  $J_{wi}$  and  $\omega_i$  show the wheel's moment of inertia and angular velocity,  $R$  is the radius of wheels,  $M_{di}$  is the torque applied

to the driving wheel by the differential's axle shaft, the braking torque is expressed by  $M_{bi}$ ,  $M$  is the control variable, the active yaw moment.

The tire's longitudinal force and lateral force are calculated by a Gim tire model (Gim and Nikravesh, 1990).

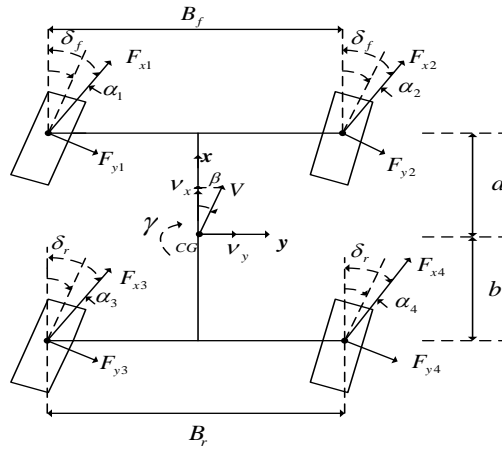


Figure 1. The steering model of a 4WS vehicle

## 2.2 Linearized Lateral Model of 4WS Vehicle

The handling stability of a 4WS vehicle during steering dynamics can be measured by two indicators: yaw rate and side slip angle of the COG if roll, pitch, and vertical dynamics are disregarded. Because  $\delta_f$  and  $\delta_r$  generally are small, their cosine values are approximately equal to 1 ( $\cos \delta_f \approx 1$ ,  $\cos \delta_r \approx 1$ ). Assuming that sideslip angle  $\beta$  was small as well and the vehicle's velocity  $V$  changed slowly, the slip angles of four tires would be derived based on  $\beta = \arctan(v_y/v_x)$  by,

$$\begin{cases} \alpha_1 = \alpha_2 \approx \beta + a\gamma/v_x - \delta_f \\ \alpha_3 = \alpha_4 \approx \beta - b\gamma/v_x - \delta_r \end{cases} \quad (2)$$

where  $\alpha_1$ ,  $\alpha_2$ ,  $\alpha_3$  and  $\alpha_4$  represent the slip angles of the front and rear tires respectively. The slip angles of the two front ties are assumed to be equal ( $\alpha_1 = \alpha_2$ ), while the situation is similar for the rear tires ( $\alpha_3 = \alpha_4$ ).

Only the lateral and yaw motion was considered, referring to Equations (1) and (2), the 2-DOF linear model could be written as,

$$\begin{cases} mV(\dot{\beta} + \dot{\gamma}) = F_{y1} + F_{y2} + F_{y3} + F_{y4} \\ I_z \dot{\gamma} = a(F_{y1} + F_{y2}) - b(F_{y3} + F_{y4}) + M \end{cases} \quad (3)$$

$$\begin{cases} F_{y1} + F_{y2} = -k_f(\beta + a\gamma/V - \delta_f) \\ F_{y3} + F_{y4} = -k_r(\beta - b\gamma/V - \delta_r) \end{cases} \quad (4)$$

where  $k_f$  and  $k_r$  indicate the synthetic steering stiffness at the front/rear axle respectively, which are equivalent to twice the stiffness on the corresponding tire. In this scenario,  $V$  is also approximate to  $v_x$  ( $V \approx v_x$ ).

According to the linear model's equations, sideslip angle and yaw rate are chosen as state variables of the system, which can be defined as  $\mathbf{x} = [\beta, \gamma]^T$ . The system's input vector is written as  $\mathbf{u} = [\delta_r, M]^T$ , which means the controller outputs two variables, rear steering angle and yaw moment. Referring to Equations (3) and (4), the state space equation of the 4WS vehicle's linear model could be described as

$$\dot{\mathbf{x}} = \mathbf{A}\mathbf{x} + \mathbf{B}_u\mathbf{u} + \mathbf{B}_\delta\delta_f \quad (5)$$

$$\text{where } \mathbf{A} = \begin{bmatrix} a_{11} & a_{12} \\ a_{21} & a_{22} \end{bmatrix} = \begin{bmatrix} -\frac{k_f + k_r}{mV} & \frac{bk_r - ak_f}{mV^2} - 1 \\ \frac{bk_r - ak_f}{I_z} & -\frac{a^2k_f + b^2k_r}{I_zV} \end{bmatrix}, \quad \mathbf{B}_u = \begin{bmatrix} b_{u11} & b_{u12} \\ b_{u21} & b_{u22} \end{bmatrix} = \begin{bmatrix} \frac{k_r}{mV} & 0 \\ -\frac{bk_r}{I_z} & \frac{1}{I_z} \end{bmatrix},$$

$$\mathbf{B}_\delta = \begin{bmatrix} b_{\delta 1} \\ b_{\delta 2} \end{bmatrix} = \begin{bmatrix} \frac{k_f}{mV} \\ \frac{ak_f}{I_z} \end{bmatrix}.$$

### 2.3 Steering Reference Model

The desired steady-state parameters had been chosen as the control target of the 4WS vehicle to enhance the manoeuvrability at lower speeds and improve tracking ability and stability at higher speeds in normal driving

scenarios. As one of the state variables, the ideal COG's slip angle should be zero to maintain the body's attitude during a turning process. Another state variable, the ideal yaw rate ( $\gamma$ ), could be viewed as a first-order inertia system response to the front steering angle ( $\delta_f$ ) as the inertia characteristic of the controlled mechanical system. Based on the above control objectives, Nagai (2002) proposed the reference ideal model of vehicle steering, which is shown as,

$$\dot{\mathbf{x}}_d = \mathbf{A}_d \mathbf{x}_d + \mathbf{B}_{\delta_d} \delta_f \quad (6)$$

$$\text{where } \mathbf{x}_d = \begin{bmatrix} \beta_d \\ \gamma_d \end{bmatrix} = \begin{bmatrix} 0 \\ \gamma_d \end{bmatrix}, \quad \mathbf{B}_{\delta_d} = \begin{bmatrix} b_{\delta_1 d} \\ b_{\delta_2 d} \end{bmatrix} = \begin{bmatrix} 0 \\ k_\gamma / \tau_\gamma \end{bmatrix}, \quad \mathbf{A}_d = \begin{bmatrix} a_{11d} & a_{12d} \\ a_{21d} & a_{22d} \end{bmatrix} = \begin{bmatrix} 0 & 0 \\ 0 & -1/\tau_\gamma \end{bmatrix}.$$

$\tau_\gamma$  is the inertia time constant and  $k_\gamma$  is the gain of the first-order system. They are derived as:

$$k_\gamma = \frac{k_0(b_{u11}a_{21} - a_{11}b_{u21}) + (b_{\delta_1}a_{21} - b_{\delta_2}a_{11})}{(a_{11}a_{22} - a_{12}a_{21})}, \quad k_0 = \frac{b_{\delta_1}a_{22} - b_{\delta_2}a_{12}}{a_{12}b_{u21} - a_{22}b_{u11}}, \quad \tau_\gamma = \frac{k_\gamma}{k_0b_{u21} + b_{\delta_2}}.$$

### 3 Steering angle observer and sliding-mode strategy design

#### 3.1 Sliding-mode control design

Since there is no steering angle sensor, the actual angle ( $\delta_f$ ) could be estimated by the output ( $\hat{\delta}_f$ ) of the steering angle observer. Then the ideal vehicle model (6) becomes as:

$$\dot{\mathbf{x}}_d = \mathbf{A}_d \mathbf{x}_d + \mathbf{B}_{\delta_d} \hat{\delta}_f \quad (7)$$

The desired state and estimated state would be solved by Equations (6) and (7). Both the desired and estimated values of sideslip angle values are zero even though there is no front-steering angle sensor.

The control error  $\mathbf{e}$  could be defined by,

$$\mathbf{e} = \mathbf{x} - \mathbf{x}_d = \begin{bmatrix} e_\beta \\ e_\gamma \end{bmatrix} = \begin{bmatrix} \beta - \beta_d \\ \gamma - \gamma_d \end{bmatrix} = \begin{bmatrix} \beta \\ \gamma - \gamma_d \end{bmatrix} \quad (8)$$

where  $e_\beta$  and  $e_\gamma$  are the errors of sideslip angle and yaw rate between their actual and ideal values,

respectively.

It's assumed that the front wheel's estimated steering angle is zero at the initial time, expressed as  $\hat{\delta}_f(0) = 0$ .

Then an adaptive law to observe and estimate the angle could be designed as:

$$\hat{\delta}_f(t) = \int_0^t \mathbf{e}^T (\mathbf{B}_\delta - \mathbf{B}_{\delta d}) d\tau \quad (9)$$

Or the adaptive law is expressed as:

$$\dot{\hat{\delta}}_f = \mathbf{e}^T (\mathbf{B}_\delta - \mathbf{B}_{\delta d}) \quad (10)$$

In addition, to account for the real driving situation, vehicle parameters change should be added in Equation (5). Thus, it is derived as:

$$\dot{\mathbf{x}} = (\mathbf{A} + \Delta\mathbf{A})\mathbf{x} + (\mathbf{B}_u + \Delta\mathbf{B}_u)\mathbf{u} + (\mathbf{B}_\delta + \Delta\mathbf{B}_\delta)\hat{\delta}_f \quad (11)$$

where,  $\Delta\mathbf{A} = \begin{bmatrix} \Delta a_{11} & \Delta a_{12} \\ \Delta a_{21} & \Delta a_{22} \end{bmatrix}$ ,  $\Delta\mathbf{B} = \begin{bmatrix} \Delta b_{u11} & 0 \\ \Delta b_{u21} & \Delta b_{u22} \end{bmatrix}$  and  $\Delta\mathbf{B}_\delta = \begin{bmatrix} \Delta b_{\delta 1} & \Delta b_{\delta 2} \end{bmatrix}^T$ .

These changes can be considered disturbing parts of the system. Therefore, Equation (11) is also expressed as:

$$\dot{\mathbf{x}} = \mathbf{A}\mathbf{x} + \mathbf{B}_u\mathbf{u} + \mathbf{B}_\delta\hat{\delta}_f + \mathbf{d}(t) \quad (12)$$

where, the perturbation matrix  $\mathbf{d}(t) = [d_1(t), d_2(t)]^T = \Delta\mathbf{A}\mathbf{x} + \Delta\mathbf{B}_u\mathbf{u} + \Delta\mathbf{B}_\delta\hat{\delta}_f$ , the  $d_1(t)$  and  $d_2(t)$  are the perturbation components on sideslip angle and yaw rate, respectively. By solving Equations (7) and (12), the error equation is obtained as:

$$\dot{\mathbf{e}} = \mathbf{A}\mathbf{e} + (\mathbf{A} - \mathbf{A}_d)\mathbf{x}_d + \mathbf{B}_u\mathbf{u} + (\mathbf{B}_\delta - \mathbf{B}_{\delta d})\hat{\delta}_f + \mathbf{d}(t) \quad (13)$$

It is assumed that the perturbation matrix is bounded and satisfies the following relation,

$$0 < |\mathbf{d}(t)| = \begin{bmatrix} |d_1(t)| \\ |d_2(t)| \end{bmatrix} \leq \boldsymbol{\psi} = \begin{bmatrix} \psi_1 \\ \psi_2 \end{bmatrix} \quad (14)$$

Where  $\boldsymbol{\psi}$  is the bound of perturbation, whose components ( $\psi_1$  and  $\psi_2$ ) are uncertain and both greater than

zero. The adaptive law of perturbation bound is defined as,

$$\begin{cases} \dot{\hat{\psi}}_1 = \varepsilon_1 e_\beta \operatorname{sgn}(e_\beta) = \varepsilon_1 |e_\beta| \\ \dot{\hat{\psi}}_2 = \varepsilon_2 e_\gamma \operatorname{sgn}(e_\gamma) = \varepsilon_2 |e_\gamma| \end{cases} \quad (15)$$

where  $\hat{\psi}_1$  and  $\hat{\psi}_2$  are estimated values of perturbation bound,  $\varepsilon_1$  and  $\varepsilon_2$  are positive bound coefficients to be determined. Under zero initial condition ( $\hat{\psi}_1(0) = 0$  and  $\hat{\psi}_2(0) = 0$ ), the estimator of disturbance bound could be written as,

$$\begin{cases} \hat{\psi}_1(t) = \int_0^t \varepsilon_1 |e_\beta| d\tau \\ \hat{\psi}_2(t) = \int_0^t \varepsilon_2 |e_\gamma| d\tau \end{cases} \quad (16)$$

To reduce or eliminate the performance impact from the parameter changes, and to enhance the system's robustness, the sliding-mode surface function was defined as the system error function, marked as  $s = e$ . The sliding mode controller based on the exponential approach law is designed as,

$$\begin{aligned} \mathbf{u} &= [\delta_r \quad M]^T \\ &= -\mathbf{B}_u^{-1} [\mathbf{K}e + \mathbf{A}e + (\mathbf{A} - \mathbf{A}_d)\mathbf{x}_d + (\mathbf{B}_\delta - \mathbf{B}_{\delta d})\hat{\delta}_f] - \mathbf{B}_u^{-1} \operatorname{diag}(\varepsilon_1 \hat{\psi}_1, \varepsilon_2 \hat{\psi}_2) \operatorname{sgn}(e) \end{aligned} \quad (17)$$

where  $\operatorname{sgn}(\cdot)$  represents the sign function and extracts the sign of the error  $e$ , the control gain matrix is  $\mathbf{K} = \operatorname{diag}(k_1, k_2)$ , both  $k_1$  and  $k_2$  are positive, and the gain matrix of switch control is related to ' $-\mathbf{B}_u^{-1} \operatorname{diag}(\varepsilon_1 \hat{\psi}_1, \varepsilon_2 \hat{\psi}_2)$ '.

### 3.2 Stability proof

The estimated value of steering angle error is defined as  $e_{\delta_f} = \hat{\delta}_f - \delta_f$ . The error vector between the disturbance bound and its estimated vector is defined as  $e_\psi = \hat{\psi} - \psi = [\hat{\psi}_1 - \psi_1, \hat{\psi}_2 - \psi_2]^T$ . The minimum

estimated coefficient of bound is described as  $\varepsilon = \min(\varepsilon_1, \varepsilon_2)$ , which is greater than zero. If the Lyapunov function is defined as,

$$V = 0.5\mathbf{e}^T\mathbf{e} + 0.5e_{\delta_f}^2 + 0.5\mathbf{e}_{\psi}^T\mathbf{e}_{\psi} \quad (18)$$

Then,

$$\begin{aligned} \dot{V} &= \mathbf{e}^T\dot{\mathbf{e}} + e_{\delta_f}\dot{e}_{\delta_f} + \mathbf{e}_{\psi}^T\dot{\mathbf{e}}_{\psi} \\ &= \mathbf{e}^T[\mathbf{A}\mathbf{e} + (\mathbf{A} - \mathbf{A}_d)\mathbf{x}_d + \mathbf{B}_u\mathbf{u} + (\mathbf{B}_{\delta} - \mathbf{B}_{\delta d})\delta_f + \mathbf{d}(t)] + (\hat{\delta}_f - \delta_f)\dot{\delta}_f + (\hat{\boldsymbol{\psi}} - \boldsymbol{\psi})^T\dot{\hat{\boldsymbol{\psi}}} \\ &= \mathbf{e}^T[\mathbf{A}\mathbf{e} + (\mathbf{A} - \mathbf{A}_d)\mathbf{x}_d - \mathbf{K}\mathbf{e} - \mathbf{A}\mathbf{e} - (\mathbf{A} - \mathbf{A}_d)\mathbf{x}_d - (\mathbf{B}_{\delta} - \mathbf{B}_{\delta d})\hat{\delta}_f - \text{diag}(\varepsilon_1\hat{\psi}_1, \varepsilon_2\hat{\psi}_2)\text{sgn}(\mathbf{e}) \\ &\quad + (\mathbf{B}_{\delta} - \mathbf{B}_{\delta d})\delta_f + \mathbf{d}(t)] + (\hat{\delta}_f - \delta_f)\mathbf{e}^T(\mathbf{B}_{\delta} - \mathbf{B}_{\delta d}) + \mathbf{e}^T\text{diag}[\varepsilon_1(\hat{\psi}_1 - \psi_1), \varepsilon_2(\hat{\psi}_2 - \psi_2)]\text{sgn}(\mathbf{e}) \\ &= -\mathbf{K}\mathbf{e}^T\mathbf{e} - \mathbf{e}^T\text{diag}(\varepsilon_1\psi_1, \varepsilon_2\psi_2)\text{sgn}(\mathbf{e}) + \mathbf{e}^T\mathbf{d}(t) \\ &\leq -\mathbf{K}\mathbf{e}^T\mathbf{e} - \varepsilon|\mathbf{e}^T|\boldsymbol{\psi} + \mathbf{e}^T\mathbf{d}(t) \\ &\leq -\mathbf{K}\mathbf{e}^T\mathbf{e} - (\varepsilon - 1)|\mathbf{e}^T|\boldsymbol{\psi} \end{aligned} \quad (19)$$

The result of the above inequality in (19) shows that if the bound coefficient  $\varepsilon$  is greater than one ( $\varepsilon = \min(\varepsilon_1, \varepsilon_2) \geq 1$ ), then,  $\dot{V} \leq 0$ . According to the concept of Lyapunov stability law, the sliding mode controller designed for 4WS is asymptotically stable under this condition.

#### 4 Numerical Simulation Result and discussion

The designed sensorless control strategy containing the sliding mode controller, an observer of the front steering angle, and a disturbance estimator was tested in MATLAB/Simulink. Figure 2 shows this control system diagram and depicts the signalling relationships between the state variables, where the control plant is simulated by a 7-DOF model while the ideal model of vehicle steering is adopted as the steering reference model. The sensorless control strategy in this paper involves coordinating ARS and DYC to settle the sideslip angle and yaw rate to their desired response. The control approach employs the sideslip angle of the COG and

the yaw rate as controlled variables. To form a close-loop control structure, the actual values of these variables are compared with the outputs of the steering reference model through measurement feedback. This comparison generates a control error vector. To address the control error, an observer is designed for the 4WS vehicles, and an estimator is used for the disturbance boundary. They provide an estimation of the front steering angle and disturbance boundary, which is then fed into the SMC controller, along with the control error. Finally, the SMC controller generates outputs that consist of the rear-wheel steering angle and the yaw moment to control the 4WS vehicle and reduce/eliminate the control errors.

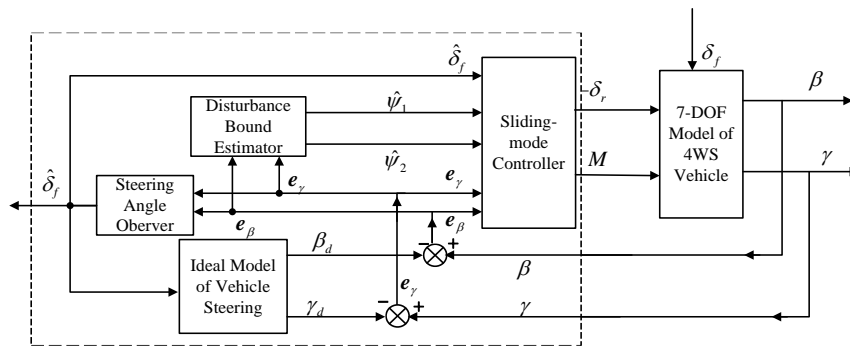


**Figure 2.** The control system diagram

The parameters of the test vehicle are listed in Table 1. Since several vehicle parameters are easily influenced by the load situation, it is assumed that moment of inertia and mass would both rise by 15%. Both the step cornering and lane change manoeuvres were carried out on a flat road to validate the control performance. The road condition is described by the road coefficient, which is expressed by  $\mu = 0.8$ . The control gain of the sliding mode controller is set by  $\mathbf{K} = \text{diag}(900, 500)$  in the simulation. Both the estimated coefficients of disturbance bound ( $\varepsilon_1$  and  $\varepsilon_2$ ) are equal to 10. In this simulation, a smoother hyperbolic function,  $\tanh(\cdot)$ , is used instead of the sign function,  $\text{sgn}(\cdot)$ , to reduce the buffeting response in the switch controller.

**Table 1.** Parameters of the 4WS vehicle

Parameter	Value/Unit	Parameter	Value/Unit
Vehicle's mass $m$	1479 (kg)	Distance from the COG to the front axle $a$	1.058 (m)
Vehicle's moment of inertia $I_z$	2731 (kg.m <sup>2</sup> )	Distance from the COG to the rear axle $b$	1.756 (m)
Synthetic cornering stiffness at front axle $k_f$	115600 (N.rad <sup>-1</sup> )	Wheelbase $L$	2.814 (m)
Synthetic cornering stiffness at rear axle $k_r$	115600 (N.rad <sup>-1</sup> )	Wheel's radius $R$	0.3075 (m)
Distance between left and right wheels $W$	1.55 (m)	Wheel's moment of inertia $J_w$	1.25 (kg.m <sup>2</sup> )

To illustrate the effectiveness of the proposed sensorless sliding mode control strategy, simulation results with a front wheel corner observer were compared with a sensor-based controller and an uncontrolled FWS vehicle. The two outputs of the ideal steering model referred to the desired value. The steering manoeuvre was implemented with the initial low and high longitudinal velocity that set to 30 and 100 km/h respectively. In the cornering manoeuvre simulation, as a steering angular input, the non-ideal step signal was applied, which begins at  $t = 0$  and leaps to 0.07 rad at  $t = 0.5$  sec. The lane change manoeuvre response will be considered under an input of a sine wave, which has a frequency of 0.25 Hz and 0.07 rad amplitude, a phase difference of 180°, and the initial time from  $t = 2$  sec. These two types of front wheel angle inputs can be described by the solid line in Figure 3 and are referred to the angular step steering and sine steering. In this way, the test for the 4WS vehicle could be grouped into four driving condition scenarios. Their response simulation curves for COG's side slip angle ( $\beta$ ), yaw rate ( $\gamma$ ), and vehicle velocity are shown in Figure 4 to Figure 6, respectively.

Regarding the estimated steering angle, as shown in Figure 3, the output of the steering angle observer exhibits an approximation of the actual steering angle in the four scenarios. During cornering manoeuvres, the estimated front steering angle (dash line) is lower than the actual value (solid line), with a steady-state error of approximately 0.02 radians. Comparable steady-state errors are also evident when comparing the amplitudes during the lane change manoeuvre. Notably, at a lower speed, a delay of 0.2 seconds is observed

in smoother curves, whereas at a higher speed, oscillations occur during the first second of the response. Overall, although there is a slight delay or oscillations, the estimation can provide a useful reflection of the steering situation, both at low and high speeds. This is one of the premises on which the performance of this sensorless control can be achieved well.

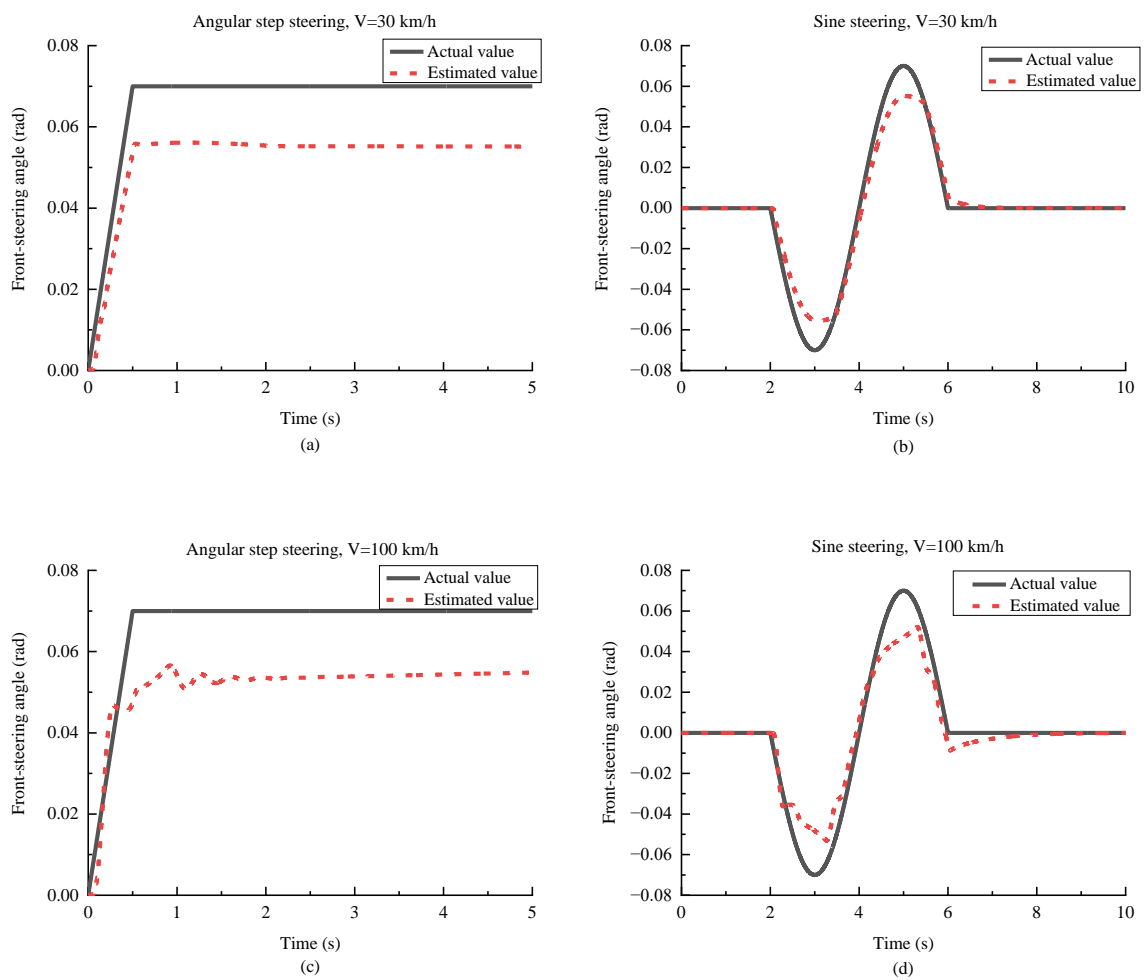


**Figure 3.** The estimated value of the front-steering angle: (a) the cornering manoeuvre at low speed, (b) the lane change manoeuvre at low speed, (c) the cornering manoeuvre at high speed, (d) the lane change manoeuvre at high speed.

In terms of the sideslip angle of COG, its desired final value should be zero according to the steering reference model. The simulation results of the sideslip angle under different driving conditions are illustrated in Figure 4. In the case of the FWS scenario, a steady-state error of approximately 0.03 radians is present at low speeds, and at high speeds, the sideslip angle exhibited a direction opposite to the steering inputs. The manoeuvring performance of the vehicle is reduced as a result, and the risk of skidding or drifting might be increased. On the other hand, the SMC scheme could achieve the desired sideslip angle value irrespective of speed or the presence of a steering angle sensor. However, upon closer observation, a tiny steady-state error was detected in the sensor-based control approach while the sensorless control method did not have this level of error. Therefore, the sensorless control method is insensitive to driving conditions and could be advantageous for ensuring the precise tracking of sideslip angles and improving the overall manoeuvrability of 4WS vehicles.

In contrast to the tracking sideslip angle, the yaw rate response is not expected to match the desired value exactly. The yaw rate represents the deflection of the vehicle about the vertical axis, and a small magnitude indicates better stability. Figure 5 depicts the yaw rate response in four driving scenarios. When the vehicle is driven at low speeds with two kinds of steering inputs, the steady-state value of the yaw rate for the 4WS vehicle is greater than that for the FWS control. This is due to one of the sliding mode controller's outputs, the yaw moment, which is applied on the 4WS vehicle. Nevertheless, both the sensorless and sensor-based controllers exhibit yaw rates that are lower than the desired value. In particular, the sensorless control strategy yields a smaller yaw rate response than the sensor-based controller. At high speeds, the yaw rate responses of the FWS vehicle exhibit massive overshoot and oscillation, which is very detrimental to vehicle stability. However, the steady-state response of the sensorless controller to the cornering manoeuvre is nearly identical to that of the sensor-based method, with only a minor overshoot of about 0.01% and a longer rise time of 1 second, which is shown in Figure 5 (c). Similarly, the yaw rate response to the lane change manoeuvre at high speeds shows comparable delays and a weak overshoot in Figure 5 (d). Figure 5 reveals that the

sensorless control strategy can overall stabilize the 4WS vehicle's yaw rate to be controlled within 0.2 rad/s at high speeds and 0.3 rad/s at low speeds, which is lower than the sensor-based method. The simulation results figure out that the sensorless approach improves the stability of the 4WS vehicle, reducing or avoiding the risk of loss of stability during lane changes at high speeds.

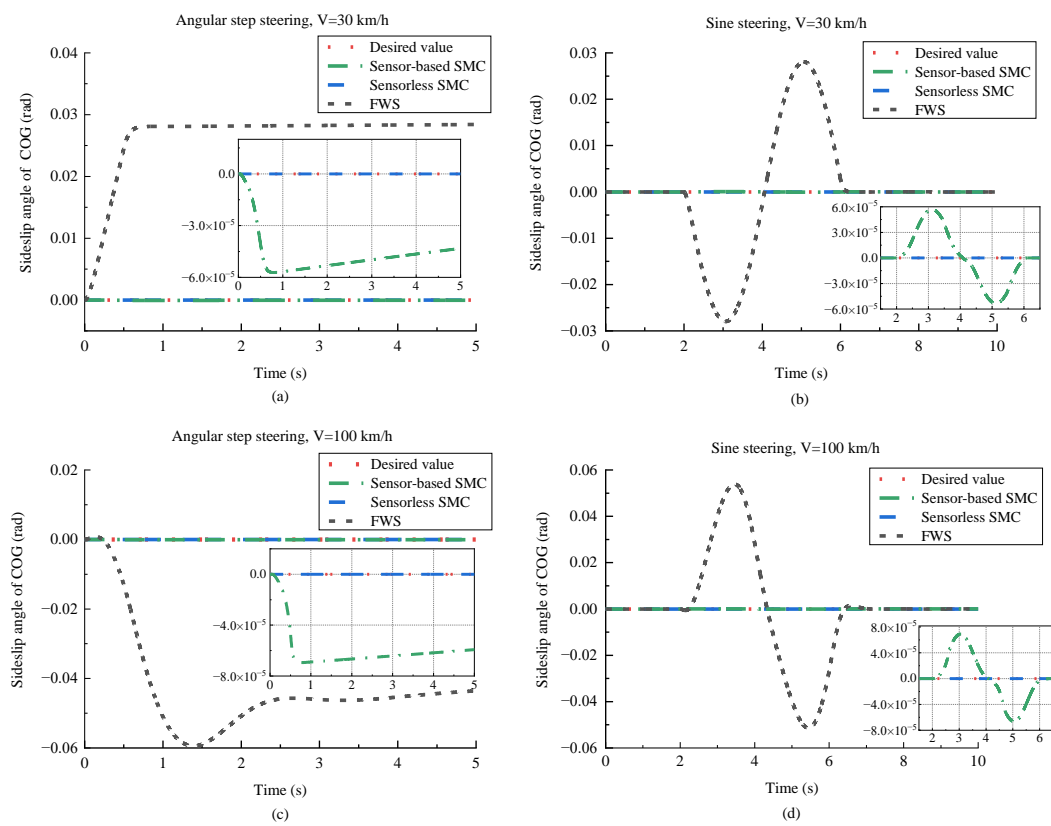


**Figure 4.** The simulation results of the sideslip angle: (a) the cornering manoeuvre at low speed, (b) the lane change manoeuvre at low speed, (c) the cornering manoeuvre at high speed, (d) the lane change manoeuvre at high speed.

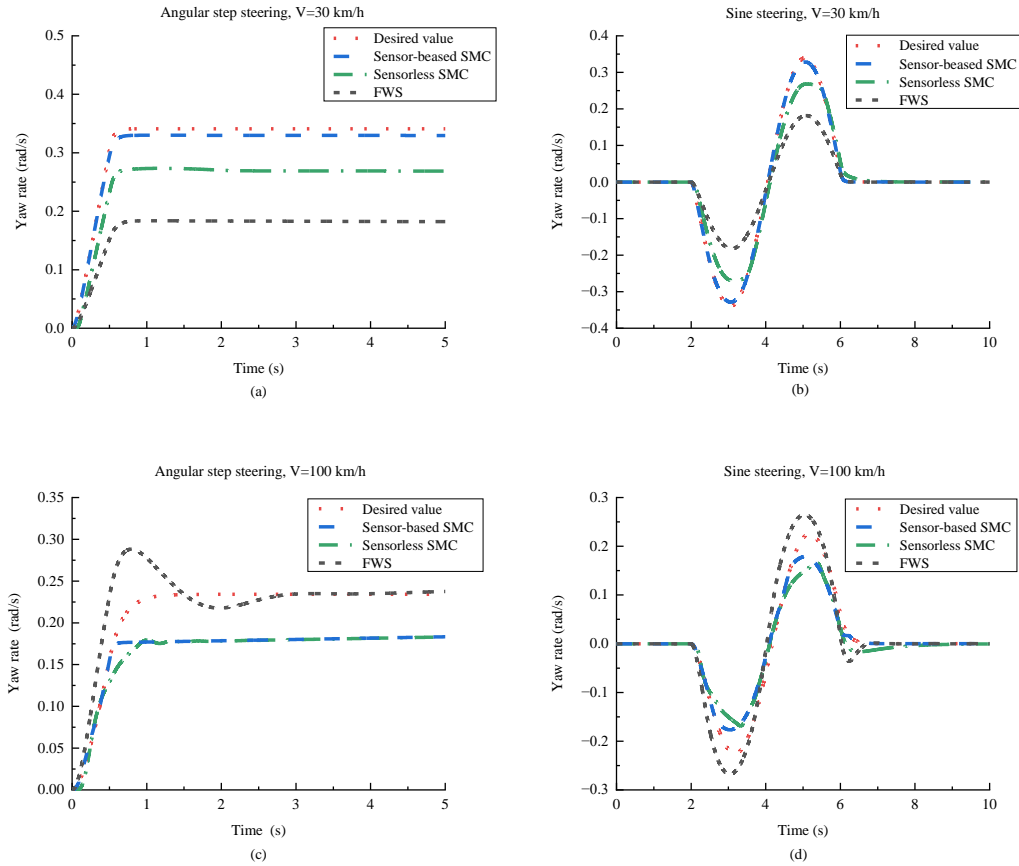


**Figure 5.** The simulation results of yaw rate: (a) the cornering manoeuvre at low speed, (b) the lane change manoeuvre at low speed, (c) the cornering manoeuvre at high speed, (d) the lane change manoeuvre at high speed.

It is noted that neither braking nor acceleration was applied during the response process. Despite this, there was still a significant reduction in velocity during and after the steering manoeuvre. The variation of the two initial velocities of the vehicle with the two types of steering input signals is demonstrated in Figure 6. The velocity decent rate under the sensorless sliding model control is only related to the type of steering input and is not sensitive to the initial velocity. For the sensorless control strategy using the angular step steering, the vehicle velocities in Figure 6 (a) and (c) decreased by about 5% of the initial

value in five seconds, while the velocities reduced by around 2% in ten seconds with the lane change manoeuvre in Figure 6 (b) and (d). Furthermore, when the initial velocity is high, the sensorless sliding mode controller is the most effective in maintaining the vehicle velocity among the three strategies. As a result, the sensorless controller's ability to maintain vehicle velocity, irrespective of the initial velocity value, makes it an attractive option for high-speed driving scenarios.

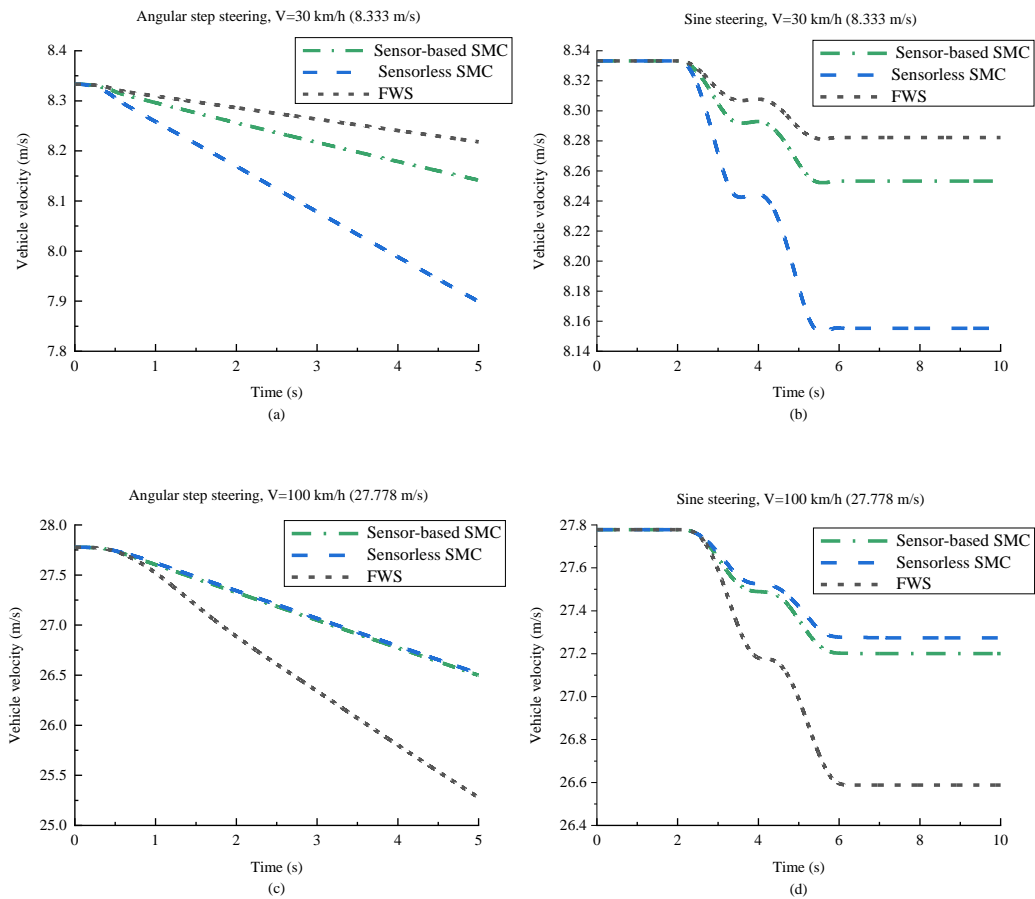


**Figure 6.** The simulation results of vehicle velocity: (a) the cornering manoeuvre at low speed, (b) the lane change manoeuvre at low speed, (c) the cornering manoeuvre at high speed, (d) the lane change manoeuvre at high speed.

In summary, the sensorless control strategy is effective in providing a useful reflection of the steering situation with some delay or oscillations, making it suitable for both low and high-speed driving conditions. It can improve the manoeuvrability of 4WS vehicles and track sideslip angles precisely. Additionally, simulation results suggest that the use of the sensorless approach enhances the stability of 4WS vehicles and reduces the risk of loss of stability during steering manoeuvres. The controller's ability to maintain vehicle velocity regardless of the initial velocity value makes it an appealing option for high-speed driving scenarios. Therefore, the sliding mode control strategy based on the steering angle observer is feasible and effective in the 4WS vehicle.

## **5 Conclusion**

In this paper, we have presented a sensorless sliding mode strategy with variable vehicle parameters, aimed at improving vehicle stability, manoeuvrability, and fault tolerance. By coordinating ARS and DYC, the sensorless control approach makes the yaw rate and sideslip angle settle to their desired status. The control system consists of a front steering angle observer, a disturbance estimator, and a sliding mode controller, which are shown to be asymptotically stable according to the Lyapunov stability law. Numerical simulation results confirmed the effectiveness of the control strategy, which demonstrated the following characteristics:

- (1) The sensorless control strategy could effectively control the COG's sideslip angle and yaw rate under different conditions of velocity and steering manoeuvre, achieving results nearly identical to those obtained with a front-steering angle sensor. is related to the estimation of the disturbance bound.
- (2) The switch control gain in the sliding mode controller can be adjusted to improve the robustness of vehicle control and counteract the negative effects of variable vehicle parameters.
- (3) The front steering angle observer could estimate the actual angle and provide useful information to

the controller, making it a reliable backup method in case of sensor failure or loss of the steering angle signal. This enhances fault tolerance and vehicle safety.

- (4) With the advancements in microprocessor control technology and the availability of specialized instruments like gyros and accelerometers, the sensorless control strategy could be implemented in practice.

Future work can explore the distribution of yaw moment to each wheel to enable a complete 4WS vehicle chassis and consider adapting to different road conditions by changing the road unevenness factor. With further research and development, we believe the sensorless control strategy could contribute to intelligent vehicle control systems.

## References

- Arslan MS and Sever M (2019) Vehicle stability enhancement and rollover prevention by a nonlinear predictive control method. *Transactions of the Institute of Measurement and Control* 41(8). SAGE Publications Ltd STM: 2135–2149. DOI: 10.1177/0142331218795200.
- Asiabar AN and Kazemi R (2019) A direct yaw moment controller for a four in-wheel motor drive electric vehicle using adaptive sliding mode control. *Proceedings of the Institution of Mechanical Engineers, Part K: Journal of Multi-body Dynamics* 233(3). SAGE Publications: 549–567. DOI: 10.1177/1464419318807700.
- Boukhari M, Chaibet A, Boukhnifer M, et al. (2018) Proprioceptive Sensors' Fault Tolerant Control Strategy for an Autonomous Vehicle. *Sensors* 18(6): 1893. DOI: 10.3390/s18061893.
- Cao Y and Qiao M (2017) Application of fuzzy control in four wheel steering control system. In: *2017 International Conference on Advanced Mechatronic Systems (ICAMechS)*, December 2017, pp. 62–66. DOI: 10.1109/ICAMechS.2017.8316551.
- Cordeiro RA, Victorino AC, Azinheira JR, et al. (2019) Estimation of Vertical, Lateral, and Longitudinal Tire Forces in Four-Wheel Vehicles Using a Delayed Interconnected Cascade-Observer Structure. *IEEE/ASME Transactions on Mechatronics* 24(2): 561–571. DOI: 10.1109/TMECH.2019.2899261.
- Du Q, Zhu C, Li Q, et al. (2022) Optimal path tracking control for intelligent four-wheel steering vehicles based on MPC and state estimation. *Proceedings of the Institution of Mechanical Engineers, Part D:*

- Journal of Automobile Engineering* 236(9). IMECHE: 1964–1976. DOI: 10.1177/09544070211054318.
- Ge G, Liu S and Xu J (2021) Research on Joint Control of Four-Wheel Steering and Electronic Differential on Account of Pavement Parameter Identification. *Automatic Control and Computer Sciences* 55(3): 222–233. DOI: 10.3103/S0146411621030044.
- Gim G and Nikravesh PE (1990) An analytical model of pneumatic tires for vehicle dynamic simulations. Part 1: Pure slips. *International Journal of Vehicle Design* 11(6). Inderscience Publishers: 589–618. DOI: 10.1504/IJVD.1990.061602.
- Hang P and Chen X (2019) Integrated chassis control algorithm design for path tracking based on four-wheel steering and direct yaw-moment control. *Proceedings of the Institution of Mechanical Engineers, Part I: Journal of Systems and Control Engineering* 233(6). IMECHE: 625–641. DOI: 10.1177/0959651818806075.
- Hang P, Chen X and Luo F (2019) LPV/ $H_\infty$  Controller Design for Path Tracking of Autonomous Ground Vehicles Through Four-Wheel Steering and Direct Yaw-Moment Control. *International Journal of Automotive Technology* 20(4): 679–691. DOI: 10.1007/s12239-019-0064-1.
- Jiang L, Wang S, Meng J, et al. (2020) Inverse Decoupling-based Direct Yaw Moment Control of a Four-wheel Independent Steering Mobile Robot. In: *2020 IEEE/ASME International Conference on Advanced Intelligent Mechatronics (AIM)*, July 2020, pp. 892–897. DOI: 10.1109/AIM43001.2020.9158953.
- Jin Xianjian, Yu Z, Yin G, et al. (2018) Improving Vehicle Handling Stability Based on Combined AFS and DYC System via Robust Takagi-Sugeno Fuzzy Control. *IEEE Transactions on Intelligent Transportation Systems* 19(8): 2696–2707. DOI: 10.1109/TITS.2017.2754140.
- Li C, Li H, Chen Y, et al. (2017) Model-based sensor fault detection and isolation method for a vehicle dynamics control system. *Proceedings of the Institution of Mechanical Engineers, Part D: Journal of Automobile Engineering* 231(2). IMECHE: 147–160. DOI: 10.1177/0954407016643225.
- Li Q, Li J, Wang S, et al. (2021) Four Wheel Steering Vehicles Stability Control Based on Adaptive Radial Basis Function Neural Network. In: *2021 33rd Chinese Control and Decision Conference (CCDC)*, May 2021, pp. 1140–1145. DOI: 10.1109/CCDC52312.2021.9602099.
- Liang Y, Li Y, Yu Y, et al. (2020) Integrated lateral control for 4WID/4WIS vehicle in high-speed condition considering the magnitude of steering. *Vehicle System Dynamics* 58(11): 1711–1735. DOI: 10.1080/00423114.2019.1645343.
- Nagai M (2002) Study on integrated control of active front steer angle and direct yaw moment. *JSAE Review* 23(3): 309–315. DOI: 10.1016/S0389-4304(02)00189-3.

- Shibahata Y (2005) Progress and future direction of Chassis control technology. *Annual Reviews in Control* 29(1): 151–158. DOI: 10.1016/j.arcontrol.2004.12.004.
- Utkin VI (1992) *Sliding Modes in Control and Optimization*. Berlin, Heidelberg: Springer Berlin Heidelberg. DOI: 10.1007/978-3-642-84379-2.
- Wang Q, Zhao Y, Deng Y, et al. (2020) Optimal Coordinated Control of ARS and DYC for Four-Wheel Steer and In-Wheel Motor Driven Electric Vehicle With Unknown Tire Model. *IEEE Transactions on Vehicular Technology* 69(10): 10809–10819. DOI: 10.1109/TVT.2020.3012962.
- Xu F-X, Xin-Hui L, Chen W, et al. (2019) Improving Handling Stability Performance of Four-Wheel Steering Vehicle Based on the  $H_2/H_\infty$  Robust Control. *Applied Sciences* 9(5). Basel, Switzerland: MDPI AG. DOI: 10.3390/app9050857.
- Yu H, Huang M and Zhang Z (2013) Direct Yaw-Moment  $H_\infty$  Control of Motor-Wheel Driving Electric Vehicle. In: *2013 IEEE Vehicle Power and Propulsion Conference (VPPC)*, October 2013, pp. 1–5. DOI: 10.1109/VPPC.2013.6671676.
- Yu S, Wang J, Wang Y, et al. (2018) Disturbance observer based control for four wheel steering vehicles with model reference. *IEEE/CAA Journal of Automatica Sinica* 5(6): 1121–1127. DOI: 10.1109/JAS.2016.7510220.
- Yuan H, Gao Y, Dai X, et al. (2017) Four-wheel-steering vehicle control via sliding mode strategy. In: *2017 6th Data Driven Control and Learning Systems (DDCLS)*, May 2017, pp. 572–577. DOI: 10.1109/DDCLS.2017.8068135.
- Zhang B, Du H, Lam J, et al. (2016) A Novel Observer Design for Simultaneous Estimation of Vehicle Steering Angle and Sideslip Angle. *IEEE Transactions on Industrial Electronics* 63(7): 4357–4366. DOI: 10.1109/TIE.2016.2544244.
- Zhang H and Zhao W (2018) Two-way  $H_\infty$  control method with a fault-tolerant module for steer-by-wire system. *Proceedings of the Institution of Mechanical Engineers, Part C: Journal of Mechanical Engineering Science* 232(1). IMECHE: 42–56. DOI: 10.1177/0954406216673672.
- Zhang Y, Wang Z, Wang Y, et al. (2022) Research on automobile four-wheel steering control system based on yaw angular velocity and centroid cornering angle. *Measurement and Control* 55(1–2). SAGE Publications Ltd: 49–61. DOI: 10.1177/00202940211035404.
- Zhao W, Qin X and Wang C (2018) Yaw and Lateral Stability Control for Four-Wheel Steer-by-Wire System. *IEEE/ASME Transactions on Mechatronics* 23(6): 2628–2637. DOI: 10.1109/TMECH.2018.2812220.